

Cytoskeletal F-actin patterns quantitated with fluorescein isothiocyanate-phalloidin in normal and transformed cells

(simian virus 40/tumor antigens/revertants/actin antibody/two-color fluorescence microscopy)

M. VERDERAME, D. ALCORTA, M. EGNOR, K. SMITH, AND R. POLLACK

Department of Biological Sciences, 813 Sherman Fairchild Center, Columbia University, New York, New York 10027

Communicated by Alex B. Novikoff, July 21, 1980

ABSTRACT Actin in cultured fibroblasts is organized into a complex set of fibers. Patterns of organization visualized with antibody to actin are similar but not identical to those visualized with fluorescein isothiocyanate-phalloidin (Fl-phalloidin), a chemical that binds to F-actin polymer with a dissociation constant of 2.7×10^{-7} M [Wulf, E., Deboen, A., Bautz, F. A., Faulstich, H. & Wieland, T. (1979) *Proc. Natl. Acad. Sci. USA* 76, 4498-4502]. Fl-phalloidin reveals that transformed cells have fewer, finer, and shorter F-actin-containing structures than do normal cells. Two-color fluorescence microscopy of single cells reveals that F-actin staining by Fl-phalloidin picks out the cytoskeletal cables more sharply than does antibody to actin, due to a reduced intracellular background fluorescence. This improved resolution permits sorting of cellular Fl-phalloidin patterns into four classes ranging in organization from 90% of the cytoplasm occupied by large cables to the absence of detectable cables. Reproducible differences in pattern distributions between normal and transformed cell lines have been quantitated. Fl-phalloidin together with rhodamine-based indirect antibody to simian virus 40 tumor antigen reveals a direct relationship between the degree of pattern change and simian virus 40 nuclear antigen expression in intermediate transformed 3T3 cell lines [Risser, R. & Pollack, R. (1974) *Virology* 59, 477-489].

Antibody to actin or transmission electron microscopy of sections cut parallel to the adherent plane reveals F-actin bundles in well-spread mammalian cells (1, 2). The bundles in normal cells are different from those in tumor cells or in many virus-transformed cell lines (3-5). In general, the difference relates to paucity and disorganization of the bundles in the abnormal cell.

A major block to quantitation of this observation has been the use of antibody to actin as the probe for actin fiber organization. Most available anti-actin antisera, even affinity-purified antisera (6), require use of a second antibody as a fluorescent probe, thereby generating an extremely complex relationship of F-actin concentration to fluorescence intensity (6). Recently, affinity-purified anti-actin has been prepared and conjugated directly to a fluorescent moiety (7). This antibody shows no nonspecific staining, and it generates patterns similar to those seen by two-step immunofluorescence. Although use of direct-conjugated antibody eliminates the problem of nonlinearity of intensity, all antisera have the drawback of intrinsic heterogeneity insofar as they are composed of a mixture of immunoglobulin molecules. In any event, quantitation of patterns with fluorescent-labeled anti-actin antibodies has depended to date upon counting the number of cells with and the number without cables (4, 5, 8). Such scores, although consistent and reproducible, totally mask the complexities of the pattern seen: two cables, however fine, make a cell as positive as a full display of thick cables filling the cytoplasm at the plane of adhesion.

The publication costs of this article were defrayed in part by page charge payment. This article must therefore be hereby marked "advertisement" in accordance with 18 U. S. C. §1734 solely to indicate this fact.

Phalloidin is a small (M_r , 788), stable compound that forms a complex with F-actin with K_d 3.6×10^{-8} M (9) and promotes the formation of F-actin from dimers and trimers of G-actin (monomeric) in solution (10). Recently, phalloidin has been specifically labeled with fluorescein (Fl-phalloidin) to produce a M_r 1250 compound that retains a strong F-actin binding affinity ($K_d = 2.7 \times 10^{-7}$ M) (11). We have screened a large number of cell lines with Fl-phalloidin to determine the quantitative effects of viral transformation on F-actin distribution pattern.

METHODS

Cells and Culture Conditions. Rat posterisis lines have been described (12, 13). They were grown in Dulbecco's modified Eagle's medium supplemented with penicillin (100 units/ml), streptomycin (100 μ g/ml), and 10% fetal calf serum (Rehatuin). Mouse cell posterisis lines have been described (14). They were grown in Dulbecco's modified Eagle's medium with penicillin (100 units/ml), streptomycin (100 μ g/ml), and 10% calf serum (GIBCO).

Mouse and rat precrisis fibroblasts were obtained from embryos and used in the third to seventh passages. They were cultured in Dulbecco's modified Eagle's medium plus 10% calf and fetal calf serum, respectively. SV80 is a simian virus 40 (SV40)-transformed human cell line obtained from W. Topp (Cold Spring Harbor Laboratory).

All cells were kept at 37°C in an atmosphere of 10% CO₂/90% air and 100% humidity. Cultures were fed twice weekly and dissociated for transfer with 0.25% trypsin/0.02% EDTA.

Fixation and Staining. Cells were plated on coverslips at a density of 2.4×10^3 cells per cm² in 10% fetal calf serum. One day later, medium was switched to 1% serum. After an additional day, cells on coverslips were fixed in 10% formalin in phosphate-buffered (pH 7.1) saline (P_i/NaCl) for 20 min, rinsed with P_i/NaCl and extracted with 1% Nonidet P-40 in P_i/NaCl for 20 min. Subsequent steps varied with the stain desired. Phalloidin concentrations were determined in concentrated stock solutions by absorbance at 300 nm (corrected for the fluorescein absorbance by measurement at 492 nm). For Fl-phalloidin staining, 10 μ l of Fl-phalloidin (1 μ g/ml in P_i/NaCl; gift of T. Wieland, West Germany) was incubated with cells at 37°C for 30 min. Coverslips were then rinsed three times in P_i/NaCl and mounted on microscope slides with Aquamount.

For double staining with antibodies to actin and Fl-phalloidin, a two-step incubation was used. First, fixed cells were incubated with rabbit anti-actin (25 μ g/ml in P_i/NaCl; gift of K.

Abbreviations: Fl-phalloidin, fluorescein isothiocyanate-phalloidin; P_i/NaCl, phosphate buffered saline; SV40, simian virus 40; T antigen, tumor antigen.

Burridge, Cold Spring Harbor Laboratory) (15) at 37°C for 1 hr. After three $P_i/NaCl$ washes, cells were then incubated with a mixture of rhodamine-conjugated goat anti-rabbit IgG (0.4 mg/ml in $P_i/NaCl$; Cappel Laboratories, Cochranville, PA) and Fl-phalloidin (1 μ g/ml). For double staining with antibody to SV40 tumor antigen (T antigen) and Fl-phalloidin, the same procedure was used but the first stain was hamster anti-T antigen (0.2 mg/ml in $P_i/NaCl$, National Institutes of Health) and the second stain was a mixture of Fl-phalloidin (1 μ g/ml) and rabbit anti-hamster IgG (0.3 mg/ml in $P_i/NaCl$, National Institutes of Health). In all cases, coverslips were rinsed three times after the second stain and mounted with Aquamount.

Immunofluorescence. Stained coverslips were examined with a Leitz Orthoplan microscope. A Zeiss Planapo X63 oil-immersion objective was coupled with a Leitz L2 exciter-barrier filter cube to reveal fluorescein or with a Leitz N2 exciter-barrier filter cube to reveal rhodamine. This apparatus completely separated the fluorescences due to rhodamine and fluorescein. Before examination, labels on all slides were blind-coded by someone other than the scorer.

Fl-phalloidin specificity for F-actin was determined in the following preincubation controls. G-actin, purified from acetone powder of chicken gizzard (refs. 16 and 17; J. Feramisco, personal communication) was converted to F-actin by the addition of KCl to a final concentration of 0.1 M. Actin preparations were mixed with Fl-phalloidin for 20 min at room temperature and then applied to coverslips of fixed 3T3 cells for 20 min at 37°C. Fl-phalloidin staining was completely blocked by F-actin at 1 mg/ml, not blocked by G-actin at 2 mg/ml, and only partially blocked by G-actin at 10 mg/ml. At this high concentration of G-actin, approximately 1% (or 0.1 mg/ml) is expected to be polymerized. Thus, staining with Fl-phalloidin was sensitive to the polymerized state of the actin. Staining by antibody to actin was completely blocked by 45-min preincubation with G-actin at 2 mg/ml.

Fl-phalloidin staining was blocked by preincubation of fixed cells with unlabeled phalloidin at 1 mg/ml (18) or the coincubation with a mixture of Fl-phalloidin (1 μ g/ml) and phalloidin (1 mg/ml). Fixed cells preincubated with phalloidin at concentrations up to 100 μ g/ml showed normal antibody staining with anti-actin. Thus, phalloidin blocked specific binding of Fl-phalloidin but not of actin antibody.

Photography. Photographs were taken with a Leitz Orthomat camera on Kodak Tri-X film developed in Microdol-X (1:3) at 22°C for 13 min. Prints were made on Kodak Polycontrast SC paper or Agfa TP6-WP, as contrast demanded.

RESULTS

Comparison of Fl-phalloidin and Anti-actin Patterns in Single Cells. Wulf *et al.* (11) have shown that Fl-phalloidin generates patterns that are qualitatively similar to those generated by antibody to actin. However, those studies did not include comparative examination of the two stains on the same cell populations. With two-color fluorescence, we were able to detect Fl-phalloidin and anti-actin patterns in the same cell. In cells of three types with widely varying cytoskeletons, the patterns were similar but not identical in any cell (Fig. 1). In the normal precrisis mouse embryo fibroblast cell, both compounds stained the large actin-containing stress fibers or cables (Fig. 1 A and B). However, the antibody stain also diffusely filled the perinuclear region of the cytoplasm as well as the nucleus (Fig. 1A); the Fl-phalloidin did not (Fig. 1B). As a result, Fl-phalloidin also revealed fine filaments in MEF whose intensity did not exceed the diffuse background of antibody-stained cells (Fig. 1B).

Patterns in the postcrisis growth-controlled cell 3T3 showed

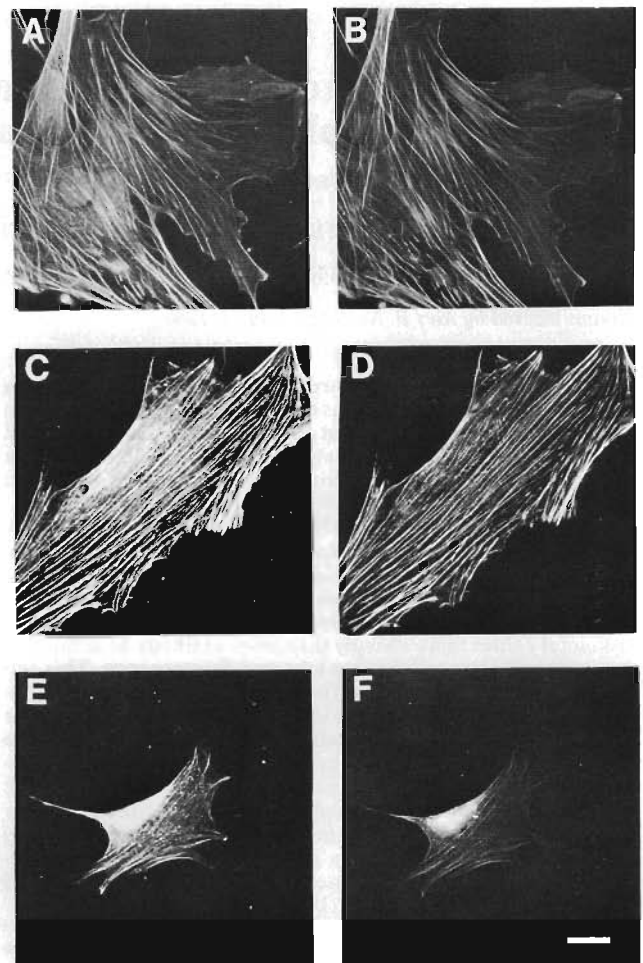


FIG. 1. Fl-phalloidin and rhodamine anti-actin patterns in MEF cells (A, B), 3T3 cells (C, D), and SV101 cells (E, F). Cell cultures were fixed, stained with rabbit antibody to actin, and then exposed to a mixture of Fl-phalloidin and goat anti-rabbit IgG. Single cells were illuminated for rhodamine (A, C, E) or fluorescein (B, D, F) and photographed. See Table 1 for properties of these cells. (Bar, 20 μ m.)

a similar difference (Fig. 1 C and D): the cables were in general thicker, but still Fl-phalloidin was capable of revealing finer cables than was the antibody. In the tumorigenic transformed SV101 (19), the antibody and Fl-phalloidin detected both a diffuse actin distribution and a multiplicity of short fine cables (Fig. 1 E and F) similar to those reported from an electron microscope study of these SV40-transformed 3T3 cells (20). Thus, Fl-phalloidin microscopy confirms a loss of size and length of actin-containing structures in these transformed cells and reveals that the structures can be replaced by thinner or shorter ones as well as by a diffuse distribution of actin.

States of Organization. The multiplicity of different Fl-phalloidin-generated patterns fell into four major classes (Fig. 2). In all cases the central portion of the cell was examined and scored. Class 1 cells have heavy distinct cables that cross more than 90% of the central area of the cell; 50% of which span the breadth of the cell. Class 2 have fine cables and at least two heavy distinct cables that enter the central half of the cell and extend more than half the breadth of the cell. Class 3 cells have only fine cables. Class 4 cells have no detectable cables in the central area but do have a diffuse fluorescence. Some class 4 cells have fine cables solely at their periphery. In addition, rounded cells and cells with radial polar cables have been seen in some cultures, but under standard conditions of culture these were not more than 10% of the total in any cell line.

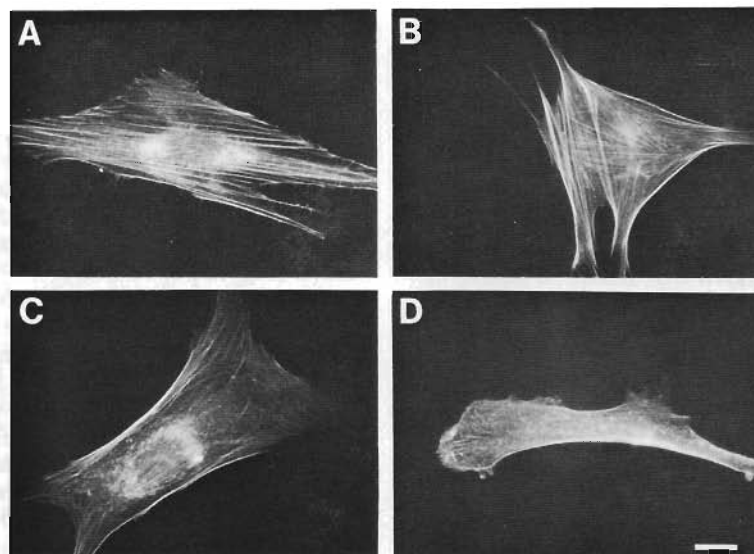


FIG. 2. Four categories of F-actin distribution used for scoring cultures stained with F1-phalloidin. (A) Category 1; >90% of cell area filled with thick cables. (B), Category 2; at least two thick cables running under nucleus, and rest of cell area filled with fine cables. (C), Category 3; no thick cables, but some fine cables present. (D) Category 4; no cables visible in the central area of the cell. (Bar, 20 μ m.)

F-actin Pattern Changes in Transformation and Reversion of Mouse Fibroblasts. Mouse cells were examined by using F1-phalloidin and distributed into categories according to the criteria in Fig. 2. For each line, some cells fell into each category. However, the distributions were reproducibly different for different cell lines. Table 1 summarizes the properties of these cell lines and also lists two single-number measures of F-actin organization derived from the histograms. The percentage of cells in classes 1 and 2 is a single score emphasizing large cables. The percentage of cells in classes 1, 2, and 3 is a single score recording all visible cables.

The precrisis mouse embryo fibroblasts and normal cell line 3T3 had F-actin pattern distributions that were undistinguishable both by histogram (Fig. 3 A and B) and by either single threshold score (Table 1). The histogram for the transformed cell SV101 had shifted due to reduction both in cells with large cables and in cells with fine cables (Fig. 3C). The SV40 T-positive partial phenotypic revertant F1SV101 (19) had many cells with fine cables, but only a few cells had regained the large cables of classes 1 and 2 (Fig. 3D).

In this set of related lines, F1-phalloidin showed that SV40 transformation reduced the size and number of F-actin-con-

Table 1. Properties of mouse, rat, and human cells

Cell	Pre/Post*	Virus	Clone of	Agar growth [†]		Tumors [‡]	F-actin cables, % [§]	
				RPE	CVI		1 + 2	1 + 2 + 3
Mouse:								
MEF	Pre	—	—	$\leq 10^{-3}$	ND	0/7	72	94
3T3	Post	—	—	$\leq 10^{-3}$	ND	0/4	76	90
SV101	Post	SV40	3T3	27	ND	5/16	11	37
F1SV101	Post	—	SV101	0.01	ND	0/2	25	82
SVR42	Post	SV40	3T3	$\leq 10^{-3}$	ND	ND	33	67
SVR63	Post	SV40	3T3	$\leq 10^{-3}$	ND	0/2	32	86
SVR13	Post	SV40	3T3	0.2	ND	0/2	39	76
SVR85	Post	SV40	3T3	10.6	ND	ND	8	22
SVR87	Post	SV40	3T3	38.6	ND	3/4	1	10
Rat:								
REF	Pre	—	—	<1	1.6	0/6	69	93
Rat 1	Post	—	—	7×10^{-3}	13	2/3	16	61
14B	Post	SV40	Rat 1	15	380	3/3	1	1
1-4	Post	—	14B	3×10^{-3}	21	0/4	4	24
3-8	Post	—	14B	4×10^{-3}	1	0/4	26	80
MCA	Post	—	1-4	5.4	4200	3/3	2	14
Human:								
SV80	Post	SV40	—	1.6	ND	0/20 [¶]	16	90

MEF, mouse embryo fibroblast; REF, rat embryo fibroblast.

* Precrisis strain or postcrisis established line.

[†] Relative plating efficiency (RPE) measured colonies >0.2 mm in diameter in agar as a percentage of the colonies on the plastic dish. Colony volume increase (CVI) measured the total increase in cell number in agar culture (14, 21–23). ND, not done.

[‡] *Nude* mice with tumors at 6 months/total animals (23, 24) injected with 10^7 cells.

[§] Data taken from histograms of F-actin pattern distribution by F1-phalloidin staining of adherent cells on coverslips; cells were divided into four classes (see Fig. 2).

[¶] SV80 is not tumorigenic in *nude* mice unless the animals are heavily irradiated (ref. 25; S. Shin, personal communication).

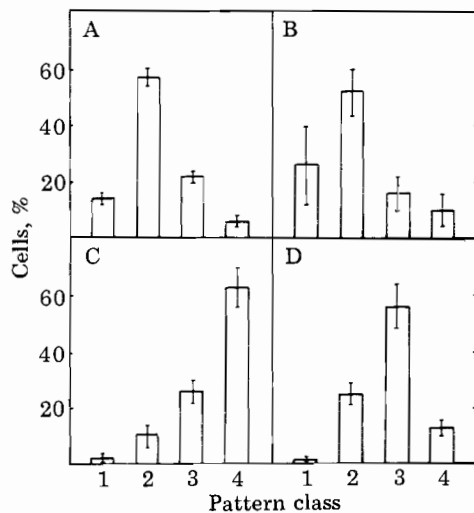


FIG. 3. F-actin pattern distribution in mouse cell lines. Cells were examined by fluorescence microscopy and sorted into one of the four categories described in Fig. 2. For each line, 200 cells were scored, on at least two coverslips each. Results are mean \pm SD for each score of each category. (A) Mouse embryo fibroblasts (MEF). (B) 3T3 normal cell line. (C) SV101-transformed cell lines. (D) F1SV101 revertant cell lines.

taining cables; partial phenotypic reversion was accompanied by an increase in number, but not a return to original cable distribution.

SV40 infection of 3T3 generates a continuum of transformed phenotypes when clones are isolated nonselectively after infection (14, 26). These phenotypes range from T-antigen-negative minimal transformants which can grow in reduced serum but not in agar, through intermediate transformants which contain small amounts of SV40 T antigens or are stable mixtures of T-antigen-positive and T-antigen-negative cells and

which grow slowly and poorly in agar, to full transformants which contain large amounts of SV40 T antigen and which grow very well in agar (14). We examined representatives of these classes of transformants (Fig. 4; Table 1). The F-actin pattern of minimal transformants and intermediate transformants deviated slightly from that of 3T3 as the major category shifted from cells with at least two large cables to cells with only fine cables (Fig. 3B; Fig. 4A and B). Full transformants were comparable to SV101, with most cells lacking any detectable cables (Fig. 4B).

F-actin Patterns and Nuclear SV40 T Antigen. The correlation of reduction in F-actin cable size and number with SV40 T antigen in these nonselected transformants suggests that T-antigen-positive cells should have fewer and finer cables than T-antigen-negative cells in the intermediate transformed lines. Using double-immunofluorescence with rhodamine-labeled antibody to T antigen and Fl-phalloidin, we examined two intermediate cell lines. The patterns of T-antigen-positive and T-antigen-negative cells within these cloned lines were significantly different, the T-antigen-positive cells having fewer and finer cables (Fig. 4D).

F-actin Pattern Changes in SV40 Transformation and Reversion of Rat Cells. We carried out a series of transformations and reversions of a rat cell line (Table 1). The growth-controlled cell line Rat 1 was used as the initial line (27, 28). From it, 14B was isolated after transformation with SV40 DNA (28); 14B contains SV40 large and small T antigens and one copy of integrated SV40 DNA (28). T-antigen-negative total phenotypic revertants 1-4 and 3-8 were isolated from 14B (29). 1-4 retained SV40 DNA; 3-8 lacked it. From 1-4, the phenotypically transformed subline MCA was isolated as a rare colony in agar (13); it, too, lacked SV40 T antigens.

The F-actin distributions of these lines closely mirrored those of the mouse cell lines (Table 1) in that in the more transformed lines the pattern was dominated by cells in classes 3 and 4. However, significant differences appeared upon a close comparison of the mouse and rat sets of cell lines.

Precrisis (REF and MEF) distributions were very close, but the postcrisis normal lines differ (Table 1). Rat 1 had many more cells in classes 3 and 4 than did 3T3. Transformed cells 14B essentially lacked cables. Both rat revertants had some cells with fine cables, and revertant 3-8 in addition had regained a considerable number of cells with large cables. Neither revertant had returned to the pattern of Rat 1. The spontaneous revertant MCA was almost devoid of cells with cables but was hardly different in this regard from its parent, the revertant line 1-4. Although the revertant 1-4 lacked T antigen (29) and was anchorage-dependent (29) and nontumorigenic (23), nevertheless it had an F-actin pattern distribution quite similar to that of the tumorigenic lines 14B and MCA.

DISCUSSION

The actin-based cytoskeletal framework of cultured fibroblasts visualized by fluorescence microscopy is formidably complex in its organization. The generally accepted criteria of cytoskeletal actin organization, which up to now have been based on work with antibodies, are now redefined in terms of the patterns generated by interaction of cellular F-actin with a chemical of totally known structure and well-described properties (9, 11, 18, 30). By binding with high affinity to native F-actin (11), Fl-phalloidin can generate patterns whose reproducibility permits quantitation.

We have chosen to quantitate F-actin patterns by distributing cells into four classes (Fig. 2). These classes expand the "plus/minus" scoring system used in previous studies (3, 4, 8) in that they generate two distinct thresholds of organization (Table 1).

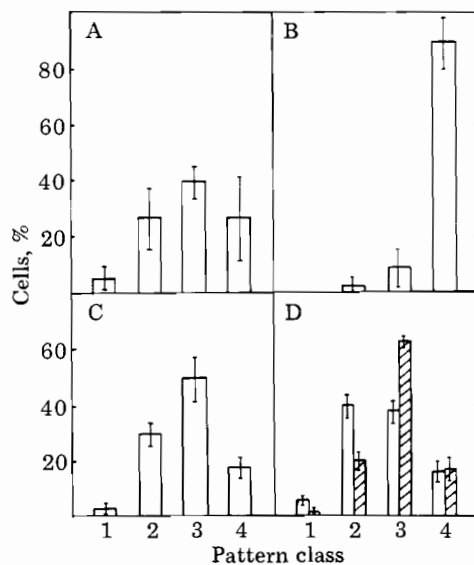


FIG. 4. F-actin patterns in nonselectively isolated SV40-transformed cell lines. Scores were obtained as in Fig. 3. (A) Minimally transformed SVR42. (B) Average scores of two fully transformant lines, SV85 and SV87. (C) Average scores of two intermediate transformed lines, SVR63 and SVR13. SV40 T antigen was absent from the minimal transformant, present in about 50% of the cells of the intermediate lines, and present in all cells of the full transformant. (D) Resolution of intermediate lines into two patterns. Open bars, T-antigen-negative intermediate cells; hatched bars, T-antigen-positive intermediate cells.

In general, the threshold that emphasizes large cables (classes 1 and 2 as percentage of total cells) reproduces quite well the fraction of "cable-positive" cells reported in studies with anti-actin (4, 5, 8, 23). Apparently, finer cables were not routinely detected in those studies. In light of the capacity of G-actin to completely block anti-actin but not F1-phalloidin, it is likely that this is at least in part the consequence of antibody recognition of fixed cellular G-actin. Because affinity-purified anti-actin that has been directly conjugated to a fluorescent moiety does not show perinuclear fluorescence (7), the perinuclear fluorescence seen here may be due to nonspecific binding.

Comparisons of patterns in similar types of cells of different species reveals significant variation. For example, the normal established mouse line 3T3 has more heavy cables than the corresponding normal established rat line Rat 1 (Table 1). The SV40-transformed cell lines SV80 (human), SV101 (mouse), and 14B (rat) all have fewer cables than their respective parents but are not similar to each other, with SV80 having the most cables and 14B having essentially no cables at all.

We used two sets of cell lines descended from each other through selection for transformation or reversion, coupled with two-color immunofluorescence, to study the role of SV40 viral gene expression in changes of F-actin patterns. The results from a set of SV40-transformed 3T3 mouse cell lines suggest that, in these lines, SV40 gene expression in a given cell (i.e., nuclear T antigen) was necessary for maximal shift in F-actin pattern (Figs. 3 and 4). The results from a set of lines descended from the SV40 DNA-transformed Rat 1 rat cell line, however, show that SV40 gene products need not be present for this pattern shift (Table 1). Both the revertant 1-4 and its spontaneous retransformed subclone MCA almost completely lack detectable F-actin cables, yet neither has any SV40 large or small T antigen. Perhaps in those cell lines the F-actin perturbation is maintained by transformation-specific molecules coded for by the host cell. We have recently shown that a 54,000-dalton protein is present in large amounts in 14B and MCA but in much smaller amounts in Rat 1 and the 14B revertants and is absent from precrisis rat fibroblasts (13).

Viral transformation is not the only perturber of F-actin pattern distribution. Our results show that establishment, the transition from precrisis cell to clonable line, can be accompanied by a significant shift: the majority of rat embryo fibroblasts are in class 2, but the majority of Rat 1 cells are in class 3 (Table 1). The cytoskeletal F-actin pattern of human fibroblasts resembles that of MEF but is changed in cells from patients with various familial colonic neoplasms (31). Such cells have patterns quite similar to those of minimal or intermediate SV40-transformed mouse 3T3 cells and an SV40-transformed human fibroblast line, SV80. Microinjection of F1-phalloidin into live cells or very gentle treatment, such as 1 min in 0.01% Nonidet P-40, followed by 1 min in the presence of F1-phalloidin at 1 μ g/ml yields images comparable to those seen here (unpublished data). Such patterns are therefore unlikely to be the result of differential extraction during the preparation of the cells.

It is likely that the classes we have used here are arbitrary boundaries within a continuum of F-actin cable length, number, and distribution. However, proof of this will require more measurements per cell than we can make by eye. Because the emitted light from F1-phalloidin is proportional to F-actin, we can couple fluorescence images to a vidicon-based digitalized image analyzer (32). In this way differences in cytoskeletal F-actin organization will result in signals that can be stored in our computer—for example, for prospective studies of cultured skin biopsy cells from persons at risk for cancer (31, 33).

We thank Dr. Theodor Wieland and Dr. A. Deboben for their gift of F1-phalloidin and Dr. K. Burridge for his rabbit anti-actin antiserum. We thank Peggy Monahan for her excellent assistance and Marisa Bolognese for her help in the preparation of this manuscript. This work was supported by National Institutes of Health Grant CA-25066 and Training Grant GM-07216 and the Josiah Macy Foundation.

- Goldman, R. D., Lazarides, E., Pollack, R. & Webster, K. (1975) *Exp. Cell Res.* **90**, 333–344.
- Lazarides, E. (1976) *J. Supramol. Struct.* **5**, 531–563.
- Pollack, R., Osborn, M. & Weber, K. (1975) *Proc. Natl. Acad. Sci. USA* **72**, 994–998.
- Edelman, G. & Yahara, I. (1976) *Proc. Natl. Acad. Sci. USA* **73**, 2047–2051.
- Tucker, R. W., Sanford, K. K. & Frankel, F. R. (1978) *Cell* **13**, 629–642.
- Osborn, M., Born, T., Koitsch, H. J. & Weber, K. (1978) *Cell* **14**, 477–488.
- Herman, I. M. & Pollard, T. D. (1979) *J. Cell Biol.* **80**, 509–520.
- McClain, D. A., Maness, P. F. & Edelman, G. M. (1978) *Proc. Natl. Acad. Sci. USA* **75**, 2750–2754.
- Faulstich, H., Schafer, A. J. & Weckauf, M. (1977) *Hoppe-Seyler's Z. Physiol. Chem.* **358**, 181–184.
- Lengsfeld, A., Low, I., Wieland, T., Dancker, P. & Hasselbach, W. (1974) *Proc. Natl. Acad. Sci. USA* **71**, 2803–2807.
- Wulf, E., Deboben, A., Bautz, F. A., Faulstich, H. & Wieland, T. (1979) *Proc. Natl. Acad. Sci. USA* **76**, 4498–4502.
- Steinberg, B., Pollack, R., Topp, W. & Botchan, M. (1978) *Cell* **13**, 19–32.
- Pollack, R., Lo, A., Steinberg, B., Smith, K., Shure, H., Blanck, C. & Verderame, M. (1980) *Cold Spring Harbor Symp. Quant. Biol.* **44**, 681–688.
- Risser, R. & Pollack, R. (1974) *Virology* **59**, 477–489.
- Burridge, K. (1976) *Proc. Natl. Acad. Sci. USA* **73**, 4457–4461.
- Feramisco, J. R. & Burridge, K. (1980) *J. Biol. Chem.* **255**, 1194–1199.
- Spudich, J. A. & Watt, S. (1971) *J. Biol. Chem.* **246**, 4866–4880.
- Wieland, T. & Faulstich, H. (1978) *CRC Crit. Rev. Biochem.* **5**, 185–260.
- Pollack, R., Green, H. & Todaro, G. J. (1968) *Proc. Natl. Acad. Sci. USA* **60**, 126–133.
- Goldman, R. D., Yerna, M. & Schloss, J. (1976) *J. Supramol. Struct.* **5**, 155–183.
- Vogel, A. & Pollack, R. (1973) *J. Cell Phys.* **82**, 189–198.
- Steinberg, B. M. & Pollack, R. (1979) *Virology* **99**, 302–311.
- Steinberg, B. M., Rifkin, D., Shin, S., Boone, C. & Pollack, R. (1979) *J. Supramol. Struct.* **11**, 539–546.
- Shin, S., Freedman, V. H., Risser, R. & Pollack, R. (1975) *Proc. Natl. Acad. Sci. USA* **72**, 4435–4439.
- Kahn, P. & Shin, S. (1979) *J. Cell Biol.* **82**, 1–16.
- Pollack, R., Risser, R., Conlon, S., Freedman, V. H., Rifkin, D. & Shin, S. (1975) in *Proteases and Biological Controls*, eds. Reich, E. & Rifkin, D. (Cold Spring Harbor Laboratory, Cold Spring Harbor, NY), pp. 885–889.
- Mishra, N. & Rayan, W. (1973) *Int. J. Cancer* **11**, 123–130.
- Botchan, M., Topp, W. & Sambrook, J. (1976) *Cell* **9**, 269–287.
- Steinberg, B., Pollack, R., Topp, W. & Botchan, M. (1978) *Cell* **13**, 19–32.
- Wieland, T. (1977) *Naturwissenschaften* **64**, 303–309.
- Kopelovich, L., Lipkin, M., Blattner, W. A., Fraumeni, J. F., Lynch, H. T., & Pollack, R. (1980) *Int. J. Cancer*, in press.
- Sobel, I., Levinthal, C. & Macagno, E. (1980) *Annu. Rev. Biophys. Bioeng.* **9**, 347–362.
- Pollack, R. & Kopelovich, L. (1979) *Methods Achiev. Exp. Pathol.* **9**, 207–230.